



Observed relation between evapotranspiration and soil moisture in the North American monsoon region

Enrique R. Vivoni,¹ Hernan A. Moreno,¹ Giuseppe Mascaro,¹ Julio C. Rodriguez,² Christopher J. Watts,³ Jaime Garatuza-Payan,⁴ and Russell L. Scott⁵

Received 16 September 2008; revised 13 October 2008; accepted 16 October 2008; published 26 November 2008.

[1] Soil moisture control on evapotranspiration is poorly understood in ecosystems experiencing seasonal greening. In this study, we utilize a set of multi-year observations at four eddy covariance sites along a latitudinal gradient in vegetation greening to infer the $ET-\theta$ relation during the North American monsoon. Results reveal significant seasonal, interannual and ecosystem variations in the observed $ET-\theta$ relation directly linked to vegetation greening. In particular, monsoon-dominated ecosystems adjust their $ET-\theta$ relation, through changes in unstressed ET and plant stress threshold, to cope with differences in water availability. Comparisons of the observed relations to the North American Regional Reanalysis dataset reveal large biases that increase where vegetation greening is more significant. The analysis presented here can be used to guide improvements in land surface model parameterization in water-limited ecosystems. **Citation:** Vivoni, E. R., H. A. Moreno, G. Mascaro, J. C. Rodriguez, C. J. Watts, J. Garatuza-Payan, and R. L. Scott (2008), Observed relation between evapotranspiration and soil moisture in the North American monsoon region, *Geophys. Res. Lett.*, *35*, L22403, doi:10.1029/2008GL036001.

1. Introduction

[2] Evapotranspiration (ET) links the surface water and energy balances with plant physiological activity, especially for water-limited ecosystems [Rodríguez-Iturbe and Porporato, 2004]. In the southwest U.S. and northwest Mexico, the strong seasonal coupling of radiation and precipitation during the North American monsoon (NAM, July–September) leads to dramatic ecosystem responses in terms of vegetation greenness [e.g., Matsui *et al.*, 2005; Watts *et al.*, 2007; Vivoni *et al.*, 2007]. While the influence of vegetation greening on the surface energy balance has been recognized, little is known of its effects on the relation between soil moisture (θ) and evapotranspiration.

[3] ET is controlled by several factors, including atmospheric, soil moisture and vegetation conditions. A common approach to simulating ET is to compute the potential evapotranspiration (ET_p) and then apply a function account-

ing for soil moisture (i.e., $ET = f(\theta)ET_p$) [e.g., Mahfouf *et al.*, 1996]. These equations typically assume time-constant plant parameters. Matsui *et al.* [2005] found that the soil moisture control on ET was a large source of uncertainty in NAM simulations, even when accounting for vegetation greening. As a result, the effects of seasonal greening on the $ET-\theta$ relation need to be further investigated for improved parameterizations in land surface models.

[4] A major difficulty in identifying the effect of vegetation dynamics on the $ET-\theta$ relation has been the lack of observations in water-limited ecosystems. The semiarid NAM region is well suited to explore the effects of vegetation greening since: (1) seasonal rainfall accounts for 40 to 70% of the annual precipitation; (2) ecosystems respond vigorously to NAM rainfall; and (3) latitudinal gradients exist in the NAM rainfall amounts and vegetation response. Here, we demonstrate that vegetation greening impacts the observed soil moisture control on evapotranspiration and evaluate its possible influence on a land surface model applied across a set of water-limited ecosystems.

2. Observations

[5] The NAM is characterized by an abrupt increase in rainfall over the southwest U.S. and northwest Mexico, starting in June or July depending on latitude. While interannual variations of NAM precipitation are substantial, regional analyses reveal spatial patterns following geographic position and elevation [e.g., Gochis *et al.*, 2007]. Figure 1 shows the percent of annual precipitation during the NAM using monthly rain gauge data [Chen *et al.*, 2002]. Note the strong seasonality, with 65 to 75% of rainfall occurring during NAM in western Mexico. Excellent correspondence is observed between precipitation and the spatial distribution of vegetation greening. This is quantified as the seasonal change (September minus June) in Normalized Difference Vegetation Index ($NDVI$), obtained from the SPOT VEGETATION sensor [Duchemin *et al.*, 2002], averaged over the 2004–2006 summers.

[6] To sample across the latitudinal gradient in vegetation greening, we use multi-year records (2004–2007) from four sites in Arizona, USA, and Sonora, Mexico, representing broad ecoregions in the NAM domain (Figure 1). Table 1 describes the study sites, which include a semiarid mesquite savanna (SR) and grassland (KN), subtropical scrubland (STS) and tropical deciduous forest (TDF). At each site, we used 30-min volumetric soil moisture (θ in % at 5 cm) and evapotranspiration (mm/day) from the eddy covariance method (EC) to derive daily values of the $ET-\theta$ relation. Soil moisture depths were selected based on available data and for consistency with tight coupling of soil moisture

¹Department of Earth and Environmental Science, New Mexico Institute of Mining and Technology, Socorro, New Mexico, USA.

²Departamento de Agricultura y Ganadería, Universidad de Sonora, Hermosillo, Mexico.

³Departamento de Física, Universidad de Sonora, Hermosillo, Mexico.

⁴Departamento de Ciencias del Agua y Medioambiente, Instituto Tecnológico de Sonora, Ciudad Obregon, Mexico.

⁵USDA Agricultural Research Service, Tucson, Arizona, USA.

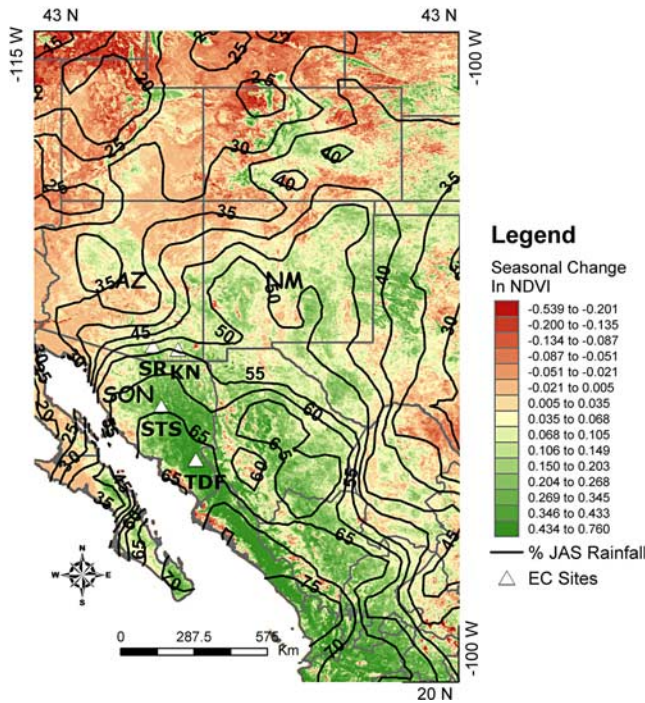


Figure 1. Spatial relation between percentage of total annual rainfall occurring during the NAM (labeled as %JAS Rainfall) and the seasonal change in *NDVI*.

control and the surface energy balance. *Watts et al.* [2007] provides descriptions of the EC method and the study sites.

3. Evapotranspiration and Soil Moisture Relation
3.1. Transition During North American Monsoon

[7] For water-limited ecosystems, a piecewise-linear equation has been proposed to depict daily evapotranspiration as [*Rodríguez-Iturbe and Porporato, 2004*]:

$$ET(\theta) = \begin{cases} 0 & 0 < \theta \leq \theta_h \\ E_w \frac{\theta - \theta_h}{\theta_w - \theta_h} & \theta_h < \theta \leq \theta_w \\ E_w + (ET_{max} - E_w) \frac{\theta - \theta_w}{\theta^* - \theta_w} & \theta_w < \theta \leq \theta^* \\ ET_{max} & \theta^* < \theta \leq n \end{cases}, \quad (1)$$

where E_w is soil evaporation, ET_{max} is unstressed evapotranspiration, θ_h , θ_w , and θ^* are volumetric soil moisture contents at the hygroscopic, wilting and plant stress thresholds, and n is soil porosity. Equation (1) is similar to the $ET = f(\theta)ET_p$ functions used in a range of land surface models [e.g., *Mahfouf et al., 1996*] and is used here only to quantify the ET - θ relation and estimate parameters. Typically, soil moisture parameters of (1) are assumed constant in time and related to soil and vegetation properties.

[8] For monsoon-dominated ecosystems, the ET - θ relation parameters may vary with time depending on vegetation greening. For example, Figure 2 presents the observed ET - θ relation for the SR site for pre-monsoon (MJ) and NAM (JAS) periods. Higher ET rates and θ typically occur during the NAM, with little overlap of the two periods. Low (high) ET and θ are coincident with minimum (maximum) greening, as indicated by low (high) *NDVI* in MJ (JAS). Note the peak *NDVI* of ~ 0.4 occurs ~ 1 month after the precipitation peak (~ 100 mm), due to the delay in biomass production. Large variations in the ET - θ relations between pre-monsoon and NAM periods also take place at the other sites, although the ET and θ ranges vary. In contrast, *Matsui et al.* [2005] only found minor differences in the simulated ET - θ relation between pre-monsoon and NAM periods, since their transpiration parameterization was severely limited at low soil moisture values.

[9] To quantify the shift in the ET - θ relation, we used a nonlinear optimization algorithm [*Gill et al., 1981*] to obtain parameters of (1) and its goodness of fit for all sites. Table 2 presents the variations in ET_{max} , E_w and θ^*/θ_{max} from pre-monsoon to NAM conditions, as well as All Data (MJJAS). Regressions of the observed data with (1) yield increases in ET_{max} and E_w and reductions in θ^*/θ_{max} as precipitation (P) and *NDVI* increase during the NAM. These trends suggest plant phenology plays a role in varying maximum ET and lowering plant stress threshold, θ^* . An example of the differences in the regressions is shown in Figure 2 for SR. At low θ (~ 2 to 6%), stressed ET in the NAM is greater than for the pre-monsoon, while unstressed ET is only observed during the NAM for high θ (~ 9 to 12%). As expected, however, equation (1) is a simplification of the observed variations of ET with θ in monsoon-dominated ecosystems.

3.2. Seasonal, Interannual and Ecosystem Variability

[10] Observed variations in the soil moisture control on ET are further explored in Figure 3, presented as the

Table 1. Study Site Characteristics

Site	Vegetation Type/Ecoregion	Location	Latitude (deg)	Longitude (deg)	Record Period
SR	Mesquite Savanna/Semidesert Grassland	Santa Rita Experimental Range, Arizona, USA	31.87°N	110.82°W	DOY 7–365 (2004) DOY 1–365 (2005) DOY 1–365 (2006)
KN	Grassland/Semidesert Grassland	Kendall Site, Arizona, USA	31.74°N	109.94°W	DOY 128–366 (2004) DOY 1–365 (2005) DOY 1–365 (2006)
STS	Subtropical Scrubland/Sinaloan Thornscrub	Rayón, Sonora, MX	29.74°N	110.54°W	DOY 199–290 (2004) DOY 152–240 (2006) DOY 189–228 (2007)
TDF	Tropical Deciduous Forest/Sinaloan Deciduous Forest	Tesopaco, Sonora, MX	27.85°N	109.30°W	DOY 192–275 (2004) DOY 151–274 (2005) DOY 151–275 (2006)

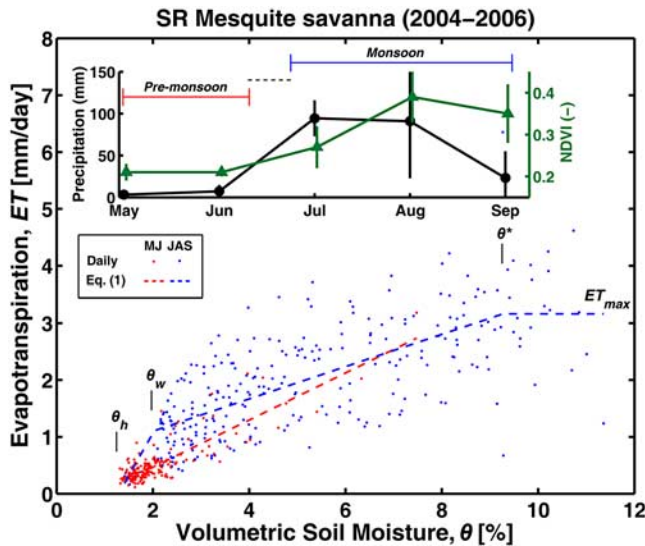


Figure 2. Daily ET (mm/day) and soil moisture (θ in %) relation at SR. Fitted equations (1) are shown as dashed lines for each period. Derived values of θ_h , θ_w , θ^* and ET_{\max} for JAS are labeled. Inset shows monthly precipitation and $NDVI$, obtained from MODIS 16-day composites. Symbols are interannual averages and bars depict ± 1 standard deviation.

regression of (1) for clarity. Figure 3a shows the seasonal evolution of the ET - θ relation for the SR site for May to September. Clearly, ET increases in time as the NAM promotes vegetation greening. Pre-monsoon conditions in May and June are characterized by low, stressed ET . The rapid onset of vegetation greening in July leads to an increase in the stressed ET , but a similar form of (1). During the peak biomass in August, a minimum in θ^* and the appearance of unstressed ET_{\max} are identified, leading to a transition in the form of (1). In September, the ecosystem experiences higher plant stress (increase in θ^*), but can sustain larger ET_{\max} due to the available plant biomass. The seasonal evolution of the ET - θ relation was also observed at the other sites, indicating that this phenomenon is widespread for monsoon-dominated ecosystems.

[11] This seasonal evolution suggests that ET_{\max} and θ^* can be directly linked to the vegetation phenology. Figure 3a (inset) presents linear regressions of monthly ET_{\max} and θ^*/θ_{\max} with monthly $NDVI_m$ for all ecosystems, indicating that ET_{\max} increases and the plant stress threshold decreases with higher $NDVI_m$. Similar regressions are shown in Figures 3b (inset) and 3c (inset) for the annual ET_{\max} and θ^*/θ_{\max} with $NDVI_{\max}$. The phenological control on ET_{\max} is significant ($R^2 = 0.51$ and 0.38 at annual and monthly scales), supporting the use of a vegetation index to modify (1) [e.g., Williams and Albertson, 2004]. Regressions between θ^*/θ_{\max} and $NDVI$ are negative, but relatively weak due to varying trends in individual ecosystems ($R^2 = 0.03$ and 0.18 at annual and monthly scales). This suggests that ecosystem-dependent stress threshold changes occur during the NAM, which are not considered in land surface models [e.g., Chen et al., 1996; Matsui et al., 2005].

[12] In addition to seasonal changes, the observed ET - θ relation has high interannual variability as shown in Figure 3b for KN and STS, which represent a gradient in vegetation greening from a grassland to a subtropical scrubland. Clearly, ET_{\max} varies from year to year, with a narrow range of 2.22 to 2.71 mm/day for KN and a wider range of 2.06 to 3.60 mm/day for STS. Interestingly, yearly changes in θ^*/θ_{\max} show opposite behavior, with a wider range at KN (0.55–0.80) and narrower changes at STS (0.77–0.86). In addition, interannual variations in the ET - θ relation are tied to total precipitation and its seasonal distribution, as this controls plant phenology. In general, wetter summers lead to higher $NDVI_{\max}$, which induces greater ET_{\max} and lower θ^*/θ_{\max} (insets for Figures 3b and 3c). This suggests these ecosystems adjust their ET - θ relation, by changes in plant biomass (ET_{\max}) and/or stress threshold (θ^*), to cope with interannual changes in NAM precipitation.

[13] To compare the ecosystems, Figure 3c presents the ET - θ relations for SR, KN, STS and TDF based on all available data. ET_{\max} increases from 2.52 mm/day at KN to 4.03 mm/day at TDF, closely following the degree of vegetation greening ($NDVI$ in Table 2). The SR and STS sites have similar ET_{\max} and θ^*/θ_{\max} perhaps due to sharing a similar vegetation type, though $NDVI$ is higher at STS. Furthermore, a progressive increase in the slope of the

Table 2. Parameters of the Observed ET - θ Relation^a

Site	Period	P (mm)	ET_{\max} (mm/day)	E_w (mm/day)	θ^*/θ_{\max}	$NDVI$	$RMSE$ (mm/day)
SR	Pre-monsoon	10.4 ± 5.1	2.97	0.44	1.00	0.21 ± 0.02	0.21
	NAM	208.4 ± 48.1	3.16	1.11	0.82	0.34 ± 0.07	0.68
	All Data	218.9 ± 52.2	3.02	0.80	0.70	0.29 ± 0.09	0.58
KN	Pre-monsoon	7.5 ± 4.9	2.35	0.36	0.88	0.19 ± 0.03	0.30
	NAM	158.3 ± 73.9	2.51	0.62	0.59	0.31 ± 0.12	0.55
	All Data	165.8 ± 70.6	2.52	0.41	0.57	0.26 ± 0.11	0.47
STS	Pre-monsoon	31.6 ± 24.6^b	–	–	–	0.24 ± 0.04	–
	NAM	301.2 ± 206.5^b	2.83	0.43	0.65	0.50 ± 0.11	0.91
	All Data	335.2 ± 254.5^b	2.83	0.43	0.65	0.38 ± 0.15	0.91
TDF	Pre-monsoon	46.4 ± 48.7^b	3.74	0.49	1.00	0.31 ± 0.03	0.67
	NAM	440.3 ± 94.5	4.74	2.12	0.83	0.72 ± 0.11	1.21
	All Data	476.9 ± 180.1^b	4.03	1.28	0.59	0.56 ± 0.22	1.17

^aThe θ_{\max} is the maximum θ for the period of interest. P and $NDVI$ depict the interannual mean ± 1 standard deviation. The root mean square error ($RMSE$) measures the goodness of fit of (1) to the observations. A dash denotes data were unavailable.

^bDenotes significant data loss.

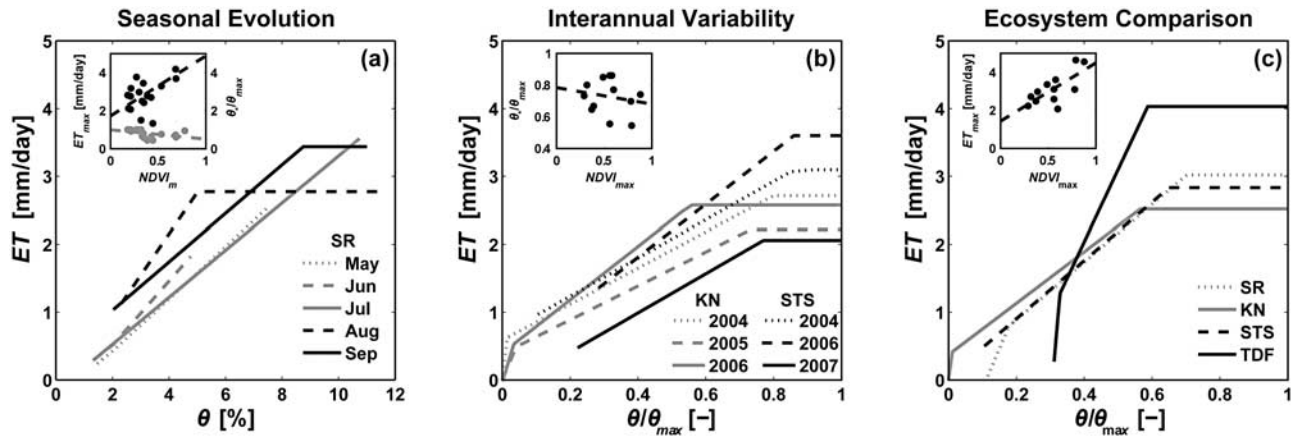


Figure 3. (a) Seasonal evolution of the ET - θ relation for SR. Inset shows regressions between ET_{\max} and $NDVI_m$ (black dots) and θ^*/θ_{\max} and $NDVI_m$ (gray dots). (b) Interannual variability of ET - θ relation for KN and STS. Inset shows the regression of annual θ^*/θ_{\max} and $NDVI_{\max}$. (c) Ecosystem comparison of the ET - θ relation for all sites. Inset shows the regression between annual ET_{\max} and $NDVI_{\max}$.

stressed ET (between θ_w and θ^*) is observed in the following order: KN, SR, STS, TDF. As a result, ecosystems with more intense greening have higher ET responses for a unit change in soil moisture under stressed conditions and can achieve higher levels of unstressed ET . Clearly, the impact of vegetation greening on the representation of the ET - θ relation should be captured in land surface models applied across the NAM region.

3.3. Comparison to a Land Surface Model

[14] To test if a land surface model represents the impact of vegetation greening on the ET - θ relation, we inspect simulations from the North American Regional Reanalysis (NARR) [Mesinger *et al.*, 2006]. NARR uses the Noah model [Chen *et al.*, 1996] to simulate land surface states and fluxes. To match the observations, we extracted daily ET (mm/day) and soil moisture in the top 0–10 cm (θ in %, valid at 5 cm) from the 32-km NARR pixels co-located at each site. We selected NARR for this comparison since: (1) the product is used to assess land-atmosphere interactions [Luo *et al.*, 2007]; (2) soil moisture control on potential ET , estimated through the Penman equation, is prescribed by a form similar to (1) [see Chen *et al.*, 1996, pp. 7254–7256 and Figure 1]; and (3) vegetation greening is captured by a monthly (interpolated to daily), 15-km $NDVI$ data set which does not account for interannual variability [Mesinger *et al.*, 2006].

[15] Figure 4a compares the ET - θ relations derived from observations (OBS) and NARR simulations at the SR site, as an example. Large differences in soil moisture (θ/θ_{\max}) indicate that NARR has a significant wet bias in the NAM region. Minimum θ for NARR vary from 12.4% (STS) to 13.0% (SR), while maximum values (θ_{\max}) are from 31.1% (KN) to 33.8% (TDF). Despite the soil moisture overestimation, NARR captures the range of observed ET (~ 0 to 5 mm/day) as well as the transition in the ET - θ relation from pre-monsoon to NAM conditions, including the increase in ET and θ . In addition, the interannual and ecosystem variations, related to vegetation greening, are consistent

with observations (not shown), suggesting improvements with respect to Matsui *et al.* [2005]. Despite these encouraging results, parameters of (1) derived from NARR differ with respect to OBS, with a trend of lower ET_{\max} and higher θ^*/θ_{\max} for NARR (Table 3).

[16] To explore this discrepancy, Figure 4b compares ET observations (ET_{OBS}) and simulations (ET_{NARR}) for 2004 at each site, selected to match the North American Monsoon Experiment [Higgins and Gochis, 2007]. Clearly, NARR over- (under-) estimates ET for days with low (high) ET_{OBS} . These important discrepancies are related to variations in the parameters of (1) for NARR. Figure 4c summarizes the OBS and NARR comparison as a conceptual diagram, highlighting that misrepresentations are likely due to not fully capturing increases in ET_{\max} and decreases in θ^*/θ_{\max} induced by vegetation greening during the NAM. The agreement between ET_{NARR} and ET_{OBS} also deteriorates from SR, KN, STS to TDF, as quantified by the SEE (Table 3). This suggests that ET simulations in NARR worsen further south in the NAM region, where seasonal precipitation and vegetation greening are more significant.

4. Conclusions

[17] Observations in four monsoon-dominated ecosystems indicate the ET - θ relation: (1) evolves during the NAM in response to plant phenology; (2) exhibits interannual changes due to vegetation differences; and (3) varies across a latitudinal gradient in vegetation greenness. Similar characteristics were observed in NARR simulations, though we found: (1) a wet bias in soil moisture; and (2) an over- (under-) estimation of ET for low (high) observations. Differences are attributed to not fully capturing the impact of vegetation greening on the ET - θ relation. Improvements could be achieved by propagating vegetation changes to the unstressed ET and plant stress threshold. Enhanced parameterizations of the ET - θ relation are necessary to constrain land-atmosphere interactions and their role in precipitation recycling in the NAM.

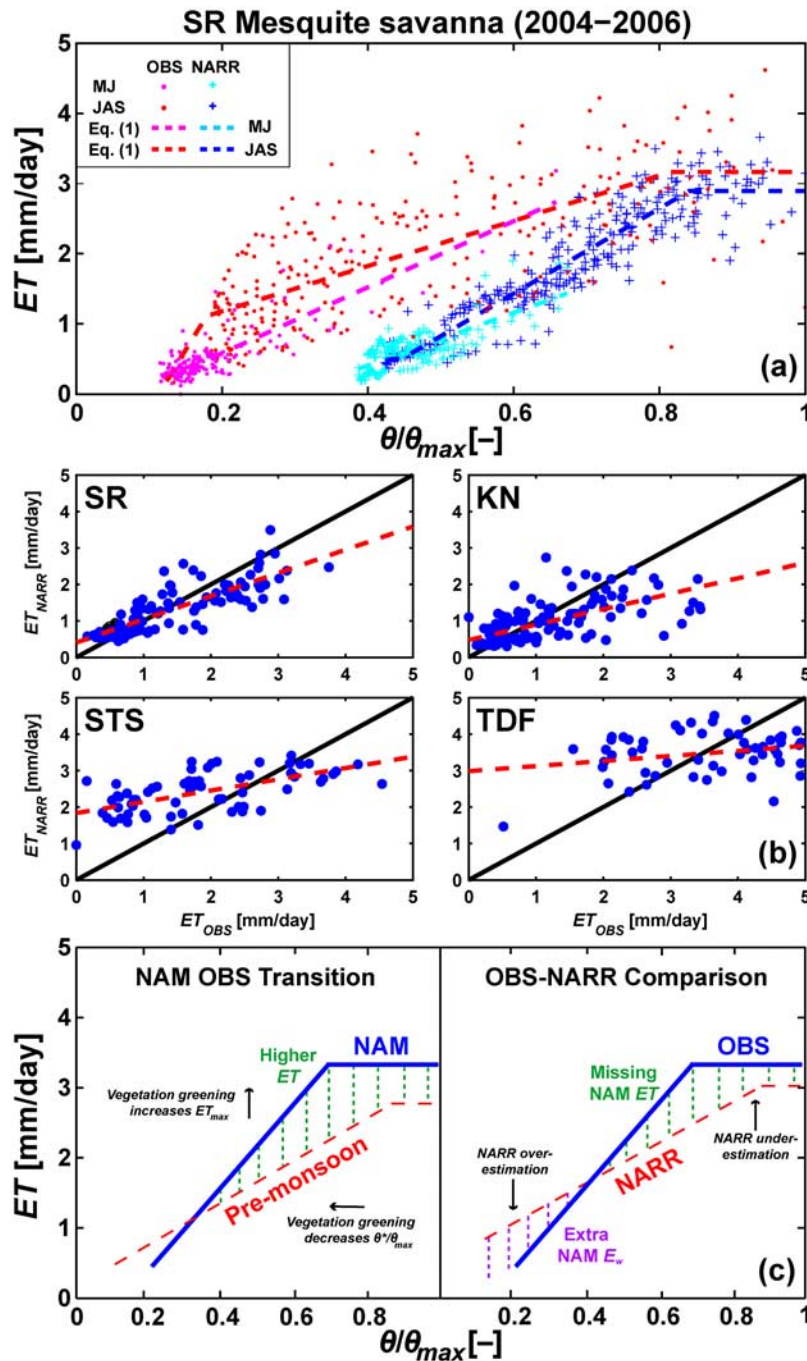


Figure 4. (a) Comparison of OBS and NARR ET - θ relations for SR. (b) Comparison of ET_{OBS} and ET_{NARR} for SR, KN, STS and TDF. Regressions of ET_{OBS} and ET_{NARR} depicted as red, dashed lines. (c) Conceptual diagrams of (left) the observed NAM transition in the ET - θ relation due to changes in ET_{max} and θ^*/θ_{max} and (right) the misrepresentation of the ET - θ relation in NARR relative to OBS. θ/θ_{max} in NARR has been scaled to match OBS.

Table 3. Parameters of the $ET-\theta$ Relation From NARR^a

Site	Period	$ET-\theta$ for NARR				ET_{OBS} vs. ET_{NARR} (2004)					
		ET_{max} (mm/day)	E_w (mm/day)	θ^*/θ_{max} (-)	$RMSE$ (mm/day)	a (-)	b (mm/day)	R^2 (-)	$RMSE$ (mm/day)	SEE (mm/day)	N (-)
SR	Pre-monsoon	1.64	0.59	1.00	0.19	0.64	0.40	0.75	0.32	0.44	149
	NAM	2.90	0.51	0.84	0.31						
	All Data	2.94	0.52	0.86	0.28						
KN	Pre-monsoon	1.23	0.48	1.00	0.15	0.42	0.47	0.40	0.42	0.65	143
	NAM	2.85	0.81	1.00	0.39						
	All Data	2.90	0.73	1.00	0.33						
STS	Pre-monsoon	1.33	0.44	1.00	0.14	0.31	1.83	0.43	0.45	1.08	67
	NAM	3.17	0.49	0.95	0.39						
	All Data	2.75	0.65	0.85	0.33						
TDF	Pre-monsoon	2.29	0.61	0.98	0.17	0.14	2.98	0.09	0.55	1.26	66
	NAM	3.50	0.59	0.75	0.66						
	All Data	3.49	1.00	0.76	0.59						

^aRegressions between ET_{OBS} and ET_{NARR} are characterized by the slope (a) and intercept (b) ($ET_{NARR} = a ET_{OBS} + b$), coefficient of determination (R^2), $RMSE$ and total days (N). For perfect agreement, $a = 1$, $b = 0$. Standard error of estimates (SEE) captures variation from 1:1 line.

[18] **Acknowledgments.** We are thankful for funding from the NOAA Climate Program Office (GC07-019) and NSF IRES Program (OISE 0553852).

References

- Chen, F., K. Mitchell, J. Schaake, Y. Xue, H.-L. Pan, V. Koren, Q. Y. Duan, M. Ek, and A. Betts (1996), Modeling of land surface evaporation by four schemes and comparison with FIFE observations, *J. Geophys. Res.*, *101*, 7251–7268.
- Chen, M., et al. (2002), Global land precipitation: A 50-yr monthly analysis based on gauge observations, *J. Hydrometeorol.*, *3*, 249–266.
- Duchemin, B., et al. (2002), Normalisation of directional effects in 10-day global syntheses derived from VEGETATION/SPOT: II. Validation of an operational method on actual data sets, *Remote Sens. Environ.*, *81*, 101–113.
- Gill, P. E., W. Murray, and M. H. Wright (1981), *Practical Optimization*, 402 pp., Academic, London, U. K.
- Gochis, D. G., et al. (2007), Spatial and temporal patterns of precipitation intensity as observed by the NAME event rain gauge network from 2002 to 2004, *J. Clim.*, *20*, 1734–1750.
- Higgins, W., and D. Gochis (2007), Synthesis of results from the North American Monsoon Experiment (NAME) process study, *J. Clim.*, *20*, 1601–1607.
- Luo, Y., et al. (2007), Relationships between land surface and near-surface atmospheric variables in the NCEP North American regional reanalysis, *J. Hydrometeorol.*, *8*, 1184–1203.
- Mahfouf, J.-F., et al. (1996), Analysis of transpiration results from the RICE and PILPS Workshop, *Global Planet. Change*, *13*, 73–88.
- Matsui, T., V. Lakshmi, and E. E. Small (2005), The effects of satellite-derived vegetation cover variability on simulated land-atmosphere interactions in the NAMS, *J. Clim.*, *18*, 21–40.
- Mesinger, F., et al. (2006), North American regional reanalysis, *Bull. Am. Meteorol. Soc.*, *87*, 343–360.
- Rodríguez-Iturbe, I., and A. Porporato (2004), *Ecohydrology of Water-Controlled Ecosystems*, 442 pp., Cambridge Univ. Press, Cambridge, U. K.
- Vivoni, E. R., et al. (2007), Variation of hydrometeorological conditions along a topographic transect in northwestern Mexico during the North American monsoon, *J. Clim.*, *20*, 1792–1809.
- Watts, C. J., et al. (2007), Changes in vegetation condition and surface fluxes during NAME 2004, *J. Clim.*, *20*, 1810–1820.
- Williams, C. A., and J. D. Albertson (2004), Soil moisture controls on canopy-scale water and carbon fluxes in an African savanna, *Water Resour. Res.*, *40*, W09302, doi:10.1029/2004WR003208.
- J. Garatuza-Payan, Departamento de Ciencias del Agua y Medioambiente, Instituto Tecnológico de Sonora, Ciudad Obregon, Sonora, 85137, Mexico.
- G. Mascaro, H. A. Moreno, and E. R. Vivoni, Department of Earth and Environmental Science, New Mexico Institute of Mining and Technology, 801 Leroy Place, MSEC 244, Socorro, NM 87801, USA. (vivoni@nmt.edu)
- J. C. Rodríguez, Departamento de Agricultura y Ganadería, Universidad de Sonora, Hermosillo, Sonora, 83000, Mexico.
- R. L. Scott, USDA Agricultural Research Service, 2000 East Allen Road, Tucson, AZ 85719, USA.
- C. J. Watts, Departamento de Física, Universidad de Sonora, Hermosillo, Sonora, 83000, Mexico.